

Establishment of a novel rat model of blast-related diffuse axonal injury

JUN-HAI ZHANG¹, JIAN-WEN GU¹, BING-CANG LI², FA-BAO GAO³, XIAO-MING LIAO⁴ and SHAO-JIE CUI¹

¹Department of Neurosurgery, The 306th Hospital of The People's Liberation Army, Beijing 100101;

²Research Institute of Surgery, State Key Laboratory of Trauma, Burns and Combined Injury, Third Military Medical University, Chongqing 400042; ³Department of Radiology and Molecular Imaging Center, West China Hospital, Sichuan University, Chengdu, Sichuan 610041; ⁴The Professional Laboratory, College of Materials Science and Engineering, Sichuan University, Chengdu, Sichuan 610065, P.R. China

Received December 21, 2016; Accepted March 5, 2018

DOI: 10.3892/etm.2018.6146

Abstract. Although studies concerning blast-related traumatic brain injury (bTBI) have demonstrated the significance of diffuse axonal injury (DAI), no standard models for this type of injury have been widely accepted. The present study investigated a mechanism of inducing DAI through real blast injury, which was achieved by performing instantaneous high-speed swinging of the rat head, thus establishing a stable animal model of blast DAI. Adult Sprague-Dawley rats weighing 150 ± 10 g were randomly divided into experimental (n=16), control (n=10) and sham control (n=6) groups. The frontal, parietal and occipital cortex of the rats in the experimental group were exposed, whereas those of the control group were unexposed; the sham control group rats were anesthetized and attached to the craniocerebral blast device without experiencing a blast. The rats were subjected to craniocerebral blast injury through a blast equivalent to 400 mg of trinitrotoluene using an electric detonator. Biomechanical parameters, and physical and behavioural changes of the sagittal head swing were measured using a high-speed camera. Magnetic resonance imaging (MRI) scans were conducted at 2, 12, 24 and 48 h after craniocerebral injury, only the experimental group indicated brain stem injury. The rats were sacrificed immediately following the MRI at 48 h for pathological examination of the brain stem using haematoxylin and eosin staining. The results indicated that 14 rats (87.5%) in the experimental group exhibited blast DAI, while no DAI was observed in the control and sham control groups, and the difference between the groups was significant ($P<0.05$). The present results indicated that this experimental design may serve to provide a stable model of blast DAI in rats.

Introduction

Explosives are major lethal weapons in modern warfare, and blast-related traumatic brain injury (bTBI), which is known as the 'signature damage' (1), is of considerable interest to researchers. bTBI is a complex injury, which includes primary (injury caused by blast waves), secondary (injury caused by high-speed shrapnel and fragments), ternary (injuries caused by the throwing, rotation and distortion of shock waves or by squeezing occurring due to the collision of objects) and quaternary (damage caused by other non-high-speed injury factors, including harmful gases, heat and light) (1).

Injury to parts of the body other than the head may also affect the evolution of brain injury, which further complicates the study of brain injury (2-11). Currently, there is no mature and stable animal model of brain blast injury (12,13), and the current major types of injury used in modelling include hydraulic, shock tube and weight drop injuries (7-21). Previously, a simple brain blast injury model using real blasts with protection of the trunk was designed by the present research group (22), and this model had aroused the attention and discussion of experts (23,24), thereby laying a reliable foundation for the present study.

Diffuse axonal injury (DAI) is a common cause of severe disabilities, vegetative states and fatality in patients with traumatic brain injury, and is typically associated with severe conditions, poor prognoses, treatment difficulties and high mortality rates (25,26). Currently, the mechanisms of DAI are considered to involve linear or angular acceleration initially generated through external forces, followed by a shearing force generated within the brain tissue, which results in axonal nerve damage or fracture and capillary damage (27,28). Previous studies have suggested a variety of animal models for the study of DAI. These include the instantaneous rotation injury model in which Gennarelli *et al* (14) designed a shearing stress-induced axonal injury model through instantaneous head rotation, which caused angular acceleration and generated shearing stress in the brain. Secondly, a hydraulic shock injury model has been created; the traumatic brain injury model was first established by Dixon *et al* (15) in 1987, who induced axonal injury through drilling in the middle

Correspondence to: Dr Jian-Wen Gu, Department of Neurosurgery, The 306th Hospital of The People's Liberation Army, 9 Anxiang Beili, Beijing 100101, P.R. China
E-mail: jianwengudoc@126.com

Key words: diffuse axonal injury, blast injury, animals, modelling

of the animal skull, causing injury to the midline structure with the impact. Meythaler *et al.* (26) applied this model in the study of DAI. A third model is Marmarou's weight drop model. Marmarou *et al.* (16) improved the weight drop injury model, which is typically used to study local craniocerebral trauma, by placing rats on foam pads, gluing a steel helmet with dental acrylic onto the skull vertex of the rat, and causing DAI by dropping a weight onto the helmet. Fourthly, a complex injury model of rotation and pounding has been proposed. Wang *et al.* (17) generated a complex injury model through the combination of the instantaneous rotation and weight drop injury models, in which DAI was created with instantaneous linear and angular acceleration to induce compound injury. Fifthly, an acceleration or deceleration injury model has also been established (18). In this model, whole brain tissue was subjected to an inertia load through accelerated or decelerated motion to generate stress in the brain tissue, which resulted in neuronal and fibre injury (18). A sixth model is the stretch injury model. Gennarelli *et al.* (14) exerted traction force directly on the nerve fibres *in vitro* to generate injuries similar to those observed in rotation, acceleration or deceleration. Seventhly, a local blast injury model was described by Garman *et al.* (19), who conducted blast exposure in rats with body shielding. Finally, a whole-body injury model has been established, in which Säljö *et al.* (20) conducted shock tube injury without any shielding. However, these models generally exhibit poor stability and do not fully represent the DAI observed in bTBI.

Based on the previous bTBI model (22), the present study investigated a means of creating DAI through real blast injury using a novel approach involving instantaneous high-speed swinging of the rat head, thereby establishing a stable animal model of blast DAI.

Materials and methods

Animals and equipment. The Experimental Animal Center of Sichuan University (Chengdu, China) provided 32 adult (1:1 ratio of male:female) Sprague-Dawley rats [animal certification number: SCXK (Chuan) 2009-09], weighing 212.2 ± 16.2 g and aged 42.2 ± 1.7 days. They were housed in polycarbonate cages with hard wood chips at a temperature of $23 \pm 2^\circ\text{C}$ and a humidity of $55 \pm 5\%$ with a 12 light/dark cycle. Food and drinking water were available *ad libitum*. After a 1-week acclimation period, the animals were subjected to the treatments. The present study was performed in strict accordance with the recommendations in the Guide for the Care and Use of Laboratory Animals of the National Institutes of Health. The animal use protocol was reviewed and the present study was approved by the Institutional Animal Care and Use Committee (IACUC) of Sichuan University.

Rats were randomly divided into experimental ($n=16$), control ($n=10$) and sham control ($n=6$) groups. The frontal, parietal and occipital cortices of rats in the experimental group were exposed to the blast; rats in the control group were not exposed to the blast, and rats in the sham control group were anesthetized as described below and attached to the craniocerebral blast device but not subjected to blasting. A self-designed craniocerebral blast injury modelling apparatus was used (Fig. 1) to fix the rats in position. The device was assembled using 19 aluminium alloy bars and 4

aluminium alloy plates, with a size of $1,000 \times 460 \times 350$ mm and a weight of 9.0 kg. Electric detonators (Chongqing Shun'an Civil Explosive Equipment Co., Ltd., Chongqing, China) and sensors were used to deliver a blast equivalent to 400 mg trinitrotoluene (containing 100 mg di-N-nonyl phthalate and 250 mg cyclotrimethylenetrinitramine; density, 1.816 g/cm^3 ; detonation velocity, 4,000 m/sec; detonation pressure, 280 kPa). Following a blast injury, the head was scanned a Bruker Biospec 70/30 7.0T magnetic resonance imaging (MRI) scanner (Bruker Corporation, Billerica, MA, USA) at the Research Center of Molecular Imaging, West China Hospital of Sichuan University. Wavebook/516A Stress Test System (IOtech, Inc.; National Instruments Corporation, Austin, TX, USA) and piezoelectric pressure sensors (113A31; Piezotronics, Inc., Depew, NY, USA) were used to the collection and analysis of shock wave parameters. A Redlake HG-LE high-speed camera device from the Red River Computer Co., Inc. (Claremont, NH, USA) at Daping Hospital, Third Military Medical University was used for the collection and analysis of head swelling parameters. A Leica RM2135 microtome (Leica Microsystems GmbH; Wetzlar, Germany) and BP3100s electronic scales (Sartorius, Tokyo, Japan) were used in the generation of paraffin sections for pathological examination. For evaluation the load-stroke curves of the spring, an electronic universal mechanical testing machine (AG-IC 20 kN; Shimadzu Corporation, Tokyo, Japan) was used at the Shimadzu Department of Material Engineering, Sichuan University.

Model preparation. Rats were anesthetized through the intraperitoneal injection of 50 mg/kg sodium pentobarbital and then fixed on a protective plate in an erect position; the head was fixed in an upward position using a carbon spring steel wire GB4357 65 Mn tooth hook (Shenzhen Nai Li Da Hardware Products Co., Ltd., Shenzhen, China; Fig. 2), and the position of the rat and the round blast window were adjusted to place the frontal, parietal and occipital parts of rats from the experimental group in the blast window, while the body below the foramen magnum, and the mouth and face above the inner canthus of the eyes were fully protected. The blast window was closed to rats in the control group, so that they were not directly exposed to the blast.

Measurement of blast waves. Based on previous experimental data (22), the distance between the piezoelectric pressure sensors, electric detonators and the exposed head of the rat were all adjusted to 10 cm, and the sensors were at the same height as the head; the sensor signals were connected to the Wavebook/516A data acquisition system. Following initiation of the electric detonator, the blast overpressure was recorded using a data acquisition system, and subsequently filtered and analysed using Origin 7.0 software (OriginLab Corporation, Northampton, MA, USA).

Measurement of biomechanical parameters of the sagittal head swing using a high-speed camera. High-speed filming was conducted perpendicular to the sagittal plane of the rats, with an image capture frequency of 1,000 times/sec, i.e., one sampling per 1 msec. According to the results of preliminary experiments, the explosion caused repeated back-forth head

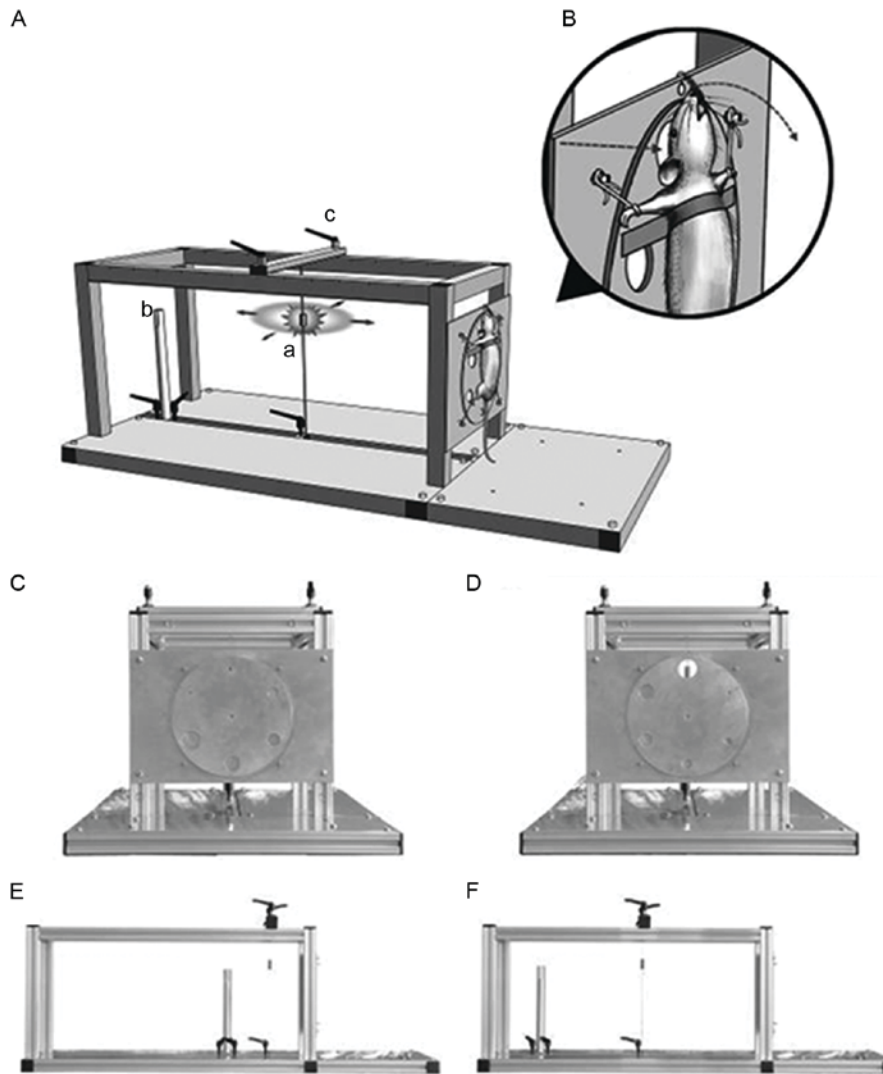


Figure 1. (A) Craniocerebral blast device. The device was assembled using 19 aluminium alloy bars and 4 aluminium alloy plates, with a size of 1,000x460x350 mm, and a weight of 9.0 kg. a, blast source (electric detonators); b, piezoelectric pressure detector fixtures; and c, locking screws for the securing of the sliding blocks. (B) Diagram of the local model. The straight arrow indicates that the explosive shock wave caused head injury through the blast window; the curved arrow indicates the direction of head swing at the time of explosion. (C and D) Six round holes with a diameter of 5-30 mm (pitch, 5 mm) were distributed evenly around the disc (diameter, 240 mm). The disc could be flipped to adjust the aperture size and change the exposure range. The blast source, piezoelectric pressure sensors and the centre of blast window were aligned. (E and F) The distance between the blast source and the blast window was adjustable to change the shock wave overpressure. The distance between piezoelectric pressure sensors and the detonator was approximately midway between the detonators and the blast window, and the overpressure of the explosion shock wave was indirectly reflected using the values measured.

swinging. The initial amplitude of the swing was the largest, and it took ~5 msec to achieve the maximum swing displacement (data not shown). Due to the limited speed of camera sampling, the sample sizes of the data were relatively small, and the credibility of the curve-fitting equation was not high; thus, it was difficult to accurately describe the head swing during explosion. Therefore, the head swinging process was divided into five successive stages (T_1 - T_5), presented in chronological order, assuming that each movement within 1 msec was a uniformly accelerated swing, and a separate examination was conducted to obtain a general understanding of the entire process. Five consecutive time periods T_1 - T_5 after the explosion were selected for parametric analysis. The five captured pictures were completely overlapped, and a line connecting the supraorbital rim with the external auditory foramen was set as the calibration line and marked as five straight lines, where the intersection of the straight lines represented the swing axis

(Fig. 2). It was initially assumed that each movement within 1 msec was a uniformly accelerated swing, and the swing angle was measured as θ_n ($n=1-5$), and according to the formulae, the equations of motion were calculated as follows:

$$\omega_n = (\theta_n - \theta_{n-1}) \times \pi \times 10^3 / 180 \text{ (rad/sec)} \quad (\theta_0 = 0)$$

$$\alpha_n = (\omega_n - \omega_{n-1}) \times 10^3 \text{ (rad/sec}^2\text{)} \quad (\omega_0 = 0)$$

$$v_{1n} = \omega_n \times r_1 \text{ (m/sec)}$$

$$v_{2n} = \omega_n \times r_2 \text{ (m/sec)}$$

ω_n is the mean angular velocity of each time period; α_n is the angular acceleration of each time period; v_{1n} is the line speed at the external auditory foramen; v_{2n} is the speed at the internal canthus; r_1 is the distance between external auditory foramen and the axis of swing; and r_2 is the distance between

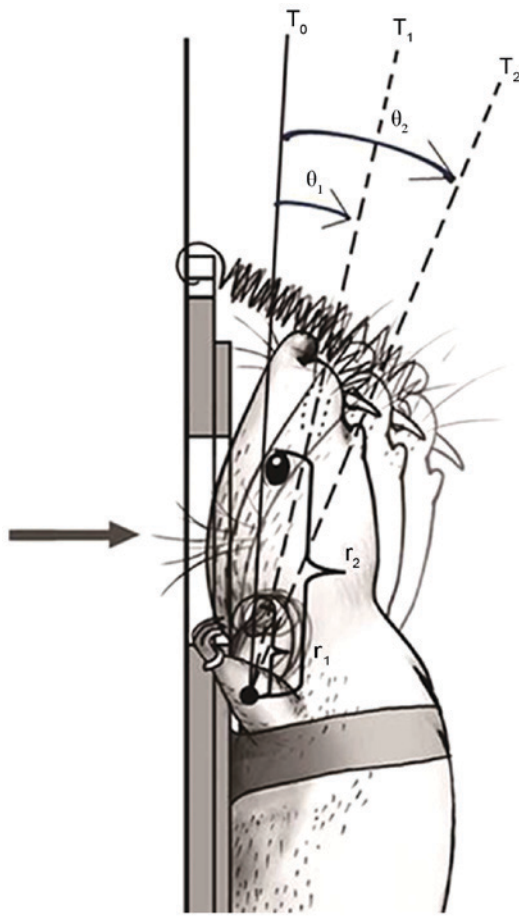


Figure 2. Schematic diagram of the head fixation and head swing. A self-made spring hanging hook was fixed to the top of the device at one end, the other end was used to hook the rat incisor. The solid line indicates the initial position of the explosion, the dotted line indicates the head position at 1 and 2 msec after explosion. The arrow shows the direction of the blast wave, and the curved arrow demonstrates the corresponding swing angle of each time period. r_1 , the distance between the external auditory foramen and the axis of swing; r_2 , distance between the inner canthus and the axis of swing; T_0 , explosion; T_1 , 1 msec after explosion; T_2 , 2 msec after explosion; θ_1 , the swing angle within 1 msec; θ_2 , the swing angle within 2 msec.

the inner canthus and the axis of swing. The swing of the external auditory foramen and that of the middle brainstem exhibited the same radius and similar linear speed, which may therefore be considered as the indirect examination of the swing of the brain stem. Similarly, the inner canthus was adopted as the reference for prefrontal movements.

Observation of clinical symptoms. The rats lost their corneal reflex when they were anesthetized. The duration of the suppression of the corneal reflex was used as an index of traumatic unconsciousness. The duration of the recovery of other reflexes was also assessed following anaesthesia. The reflexes were assessed according to the methodology of Fijalkowski *et al* (29). The following changes were also assessed: Number of cases of respiratory arrest, spontaneous breathing recovery time, number of cases of seizures or convulsions in the limbs after injury.

MRI T2 sequence scanning of the head. MRI of the head was conducted four times at 2, 12, 24 and 48 h after injury. Each rat

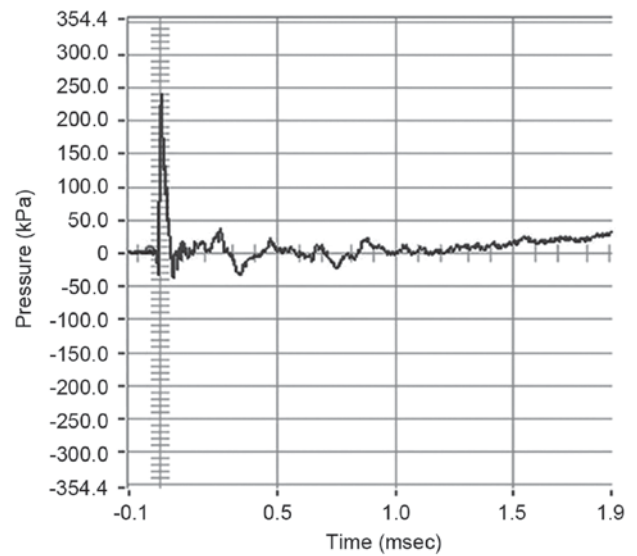


Figure 3. Waveform and composition of blast waves. The peak blast pressure value was 241.27 kPa, with a duration of ~ 0.048 msec.

was anesthetized with isoflurane (2-3%) in a small container and maintained with a mixture of 100% oxygen and isoflurane (1-2%) during the MRI scan. The body temperature was kept constant using a heating blanket at 37°C monitored with a rectal temperature probe. Each animal was placed prone in a surface coil. The ECG signal was obtained from two subcutaneous copper needles loaded in the left forelimb and hind limb. Respiration signals were acquired from a respiratory pillow (SA Instruments Inc., Stony Brook, NY, USA) under the rat. Images were recorded using a 7T MRI scanner with a volume coil (outer diameter, 44 mm; inner diameter, 23 mm) and ParaVision 5.0 software (Bruker Corporation). The MRI sequences included RARE-T2 (repetition time, 3,000 msec; echo time, 45 msec; slice thickness, 1 mm; field of view, 18 mm; matrix, 256x256).

Pathological examination of brain tissue. The rats were decapitated while still anesthetized immediately following the final MRI examination at 48 h, and a rapid craniotomy was performed to assess the general traumatic craniocerebral injury. Specimens of brain stem tissue were extracted and subjected to 10% formalin-fixation at room temperature for 48 h, dehydration with different concentrations of ethanol, vitrification with xylene and embedding in paraffin. Subsequently, 5- μ m slices were obtained and subjected to hematoxylin staining for 5 min at room temperature and eosin staining for 20 sec at room temperature and observed using light microscopy.

Statistical analysis. All statistical analyses were performed using SPSS version 16.0 software (SPSS, Inc., Chicago, IL, USA). Continuous variables are presented as the mean \pm standard deviation and categorical variables are presented as absolute value with the percentage in parentheses. Fisher's exact test was used to compare the rates of respiratory arrest and short convulsions in the limbs among the three groups. One-way analysis of variance followed by least significant difference tests were used to compare the different

Table I. Parameters of blast overpressure.

Groups	Peak pressure (kPa)	Rise time (msec)	Duration (msec)	Blast impulse (Pa.sec)
Control	238.86±18.34	0.014±0.004	0.048±0.004	32.67±1.59
Sham control	239.16±13.25	0.012±0.004	0.039±0.002	31.23±1.39
Experimental	240.52±17.54	0.013±0.005	0.051±0.003	30.55±2.09

One-way analysis of variance followed by least significant difference tests were used to analyse the significance of differences among the three groups. No significant differences in peak pressure or blast impulse were detected between the experimental and control groups or experimental and sham groups. Data are presented as the mean ± standard deviation.

study groups with regard to continuous variables, including the peak pressure and rise time. The frequencies of categorical variables were compared using Pearson χ^2 or Fisher's exact test, when appropriate. $P < 0.05$ was considered to indicate a statistically significant difference.

Results

Test of detonator blast. The waveform and composition of the blast waves is shown in Fig. 3. Analysis of the results demonstrated that the parameters of blast exposure, including peak pressure and blast impulse were relatively constant among the three groups ($P > 0.05$; Table I).

Spring parameters. The detailed parameters of the spring and the elastic are presented in Fig. 4. The stretching length of the spring was in the 0-24 mm range at explosion, and this distance in the load-stroke curves were almost in a straight line, indicating a stable and reliable spring tension.

Biomechanical parameters of the sagittal head swing. No obvious head swing was noted in the control group at the instantaneous moment of explosion; a curved head swing was observed at the sagittal plane in the control group, and the swing axis was roughly at the cervical-thoracic junction (Fig. 2). The five successive stages (T_1 - T_5) of the head swinging process were analyzed. The mean angular velocity, angular acceleration and line speed at the external auditory foramen are presented in Table II. The measurement of the biomechanical parameters of the head swings during the explosion demonstrated that the swing went through an acceleration-deceleration cycle. The momentary head swing caused the non-linear acceleration-deceleration of brain tissues, inducing shear stress perpendicular to the swing axis. The amount of the shear stress is associated with the swing radius, the weight and density of the brain tissue. This hypothesis was confirmed through measurements of the line speed at the external auditory foramen and inner canthus, which revealed differences in the swing radius. The line speeds of the middle brain stem (the external auditory foramen) and prefrontal area (the internal canthus) were significantly different, with the latter speed ~3 times that of the former (Table II). Using time as the abscissa and the mean angular velocity and angular acceleration as the vertical axis, a Cartesian coordinate system was established and used to monitor the corresponding data points.

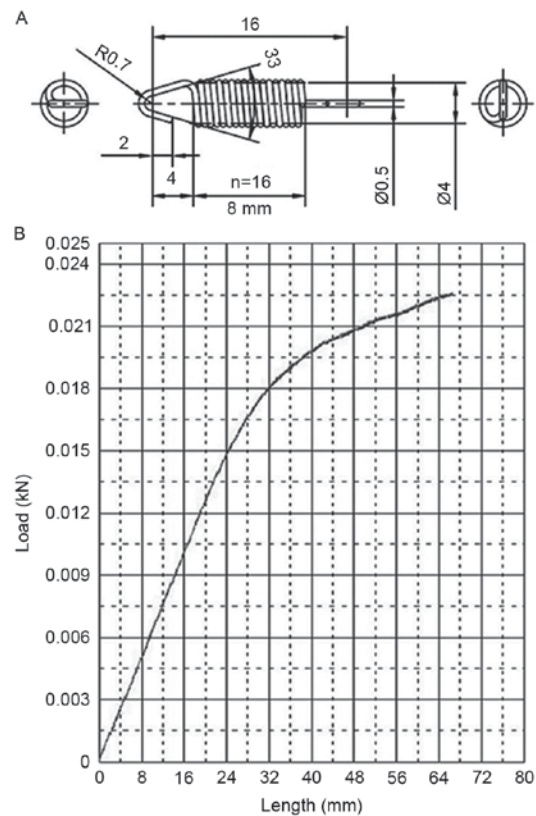


Figure 4. (A) Parameters of the size of the teeth-fixation spring hook (mm) and (B) the load-stroke curves of the spring. Stretching length of the spring was in the 0-24 mm range at explosion, and the load-stroke curves were almost in a straight line, which indicated a stable and reliable spring tension.

Clinical observation. The number of cases of brief respiratory arrest, mean recovery time of spontaneous breathing, number of cases of short convulsions in the limbs, and mean duration from anaesthesia to the recovery of the corneal reflex of the rats in the experimental group were significantly higher than those of the rats in the control group ($P < 0.05$; Table III).

MRI T2 sequence scanning of rat heads. Complete skulls were observed in the three groups, with no evident fracture, displacement or compression. At 2 h after injury, abnormal brain signals in the injured regions of rats in the experimental group were detected, and the signal change was most evident at 24 h after injury; however, no marked difference was observed between 48 and 24 h after injury in the experimental

Table II. Measurement of the biomechanical parameters of the head swing in the experimental group (n=16).

Time period	T ₁	T ₂	T ₃	T ₄	T ₅
Mean angular velocity (rad/sec)	160.2±4.3	240.3±3.8	236.8±4.1	168.2±3.7	10.3±2.2
Mean angular acceleration (krad/sec ²)	161.7±6.5	60.9±4.9	-58.9±5.1	-115.4±5.4	-202.3±9.5
Line speed at the external auditory foramen (m/sec) ^a	4.038±0.015	6.274±0.021	5.978±0.019	4.286±0.023	0.233±0.011
Speed at the internal canthus (m/sec) ^b	12.836±0.034	19.154±0.023	17.648±0.017	11.197±0.018	0.522±0.013

Values represent the mean ± standard deviation. ^aDistance between external auditory foramen and the swing axis was ~0.02 m; ^bdistance between the inner canthus and the swing axis was ~0.06 m. T₁-T₅ are five consecutive time periods following the explosion.

Table III. Clinical observation of rats.

Group	Respiratory arrest, n (%)	Mean recovery time of spontaneous breathing (sec)	Short convulsions in the limbs, n (%)	Recovery time of corneal reflex from anaesthesia (h)
Control	1 (10)	2.2±0.1	1 (10)	1.2±0.2
Sham control	0 (0)	0	0 (0)	1.3±0.1
Experimental	13 (81.3) ^{a,b}	8.6±0.2 ^{a,b}	12 (75) ^{a,b}	12.5±0.2 ^{a,b}

Fisher's exact test was used to compare the rates of respiratory arrest and short convulsions in the limbs among the three groups. ^aP<0.05 vs. the control group. ^bP<0.05 vs. the sham control. One-way analysis of variance followed by least significant difference tests were used to analyse the significance of differences in the average recovery time of spontaneous breathing and duration from anaesthesia to the recovery of corneal reflex among the three groups.

group. The results at 24 h indicated 14 cases of mixed signals at the upper dorsolateral brainstem in the experimental group, of which 6 cases exhibited contusions at the frontal cortex and top ventrolateral cerebellum (Fig. 5); furthermore, 1 case of a contusion at the frontal cortex was observed in the control group.

Histopathological examination of rat brain stems. The pathological results obtained in the experimental group were 2 cases of basal cell subarachnoid haemorrhage, 6 cases of focal brain contusions and 14 cases of diffuse swelling and congestion of the brain stem, with marked regional damage in the upper dorsolateral brainstem. The following morphological changes were observed using microscopy: Triangular, hyperchromatic nerve cell nuclei in the brainstem injury zone, with a thin cell body (Fig. 6A); and capillary congestion and expansion, sedimentation of erythrocytes and peripheral oedema (Fig. 6B). Conversely, the brain stems obtained from the control and sham control groups were normal.

Discussion

Although there are a variety of animal models of DAI, it is widely accepted that DAI is caused through shear stress, and this injury occurs almost ubiquitously throughout bTBI, which suggests an association of bTBI with DAI (30). Based on this understanding, the present study improved upon a previously investigated rat brain blast injury model (22) that caused rat head swinging with a detonator explosion shock wave in order to generate shearing stress, and subsequently induce DAI.

The present study model included a range of characteristics. Firstly, the model allowed for simulation of the real clinical traumatic brain blast injury. In the previous DAI models, the instantaneous rotation, hydraulic shock, weight drop, rotation and pounding, acceleration or deceleration injury were unable to completely reproduce traumatic brain blast injury, which made it difficult to conduct research on the occurrence of DAI at the moment of craniocerebral blast injury. Therefore, in the present study, the explosion of an electric detonator was used to cause injury. Furthermore, the present study presented a simplified model for evaluating the complex mechanisms of injury. The initiation of the electric detonator ensured that no fragment-induced injuries occurred within the effective injury distance, which minimized the possibility of secondary injury. Additionally, fixation of the limbs of the experimental animals avoided ternary injury, and the masking exposure method, where only the head was exposed to injury, effectively protected other parts of the rat, thus avoiding the possibility of brain injury induced through the chest, abdominal squeezing or damage to other organs, and reduced quaternary injury. In addition, reproduction of the present study model is simple and economical, and the modelling apparatus itself is removable and easily assembled.

Shearing force has an important role in the development of DAI and is associated with acceleration, which varies according to the shape and weight of the animal. Due to rat anatomical features, including a short neck and low weight, the shearing force from whole exposure injury on rats is far less compared with the exposure to humans (17). Thus, certain

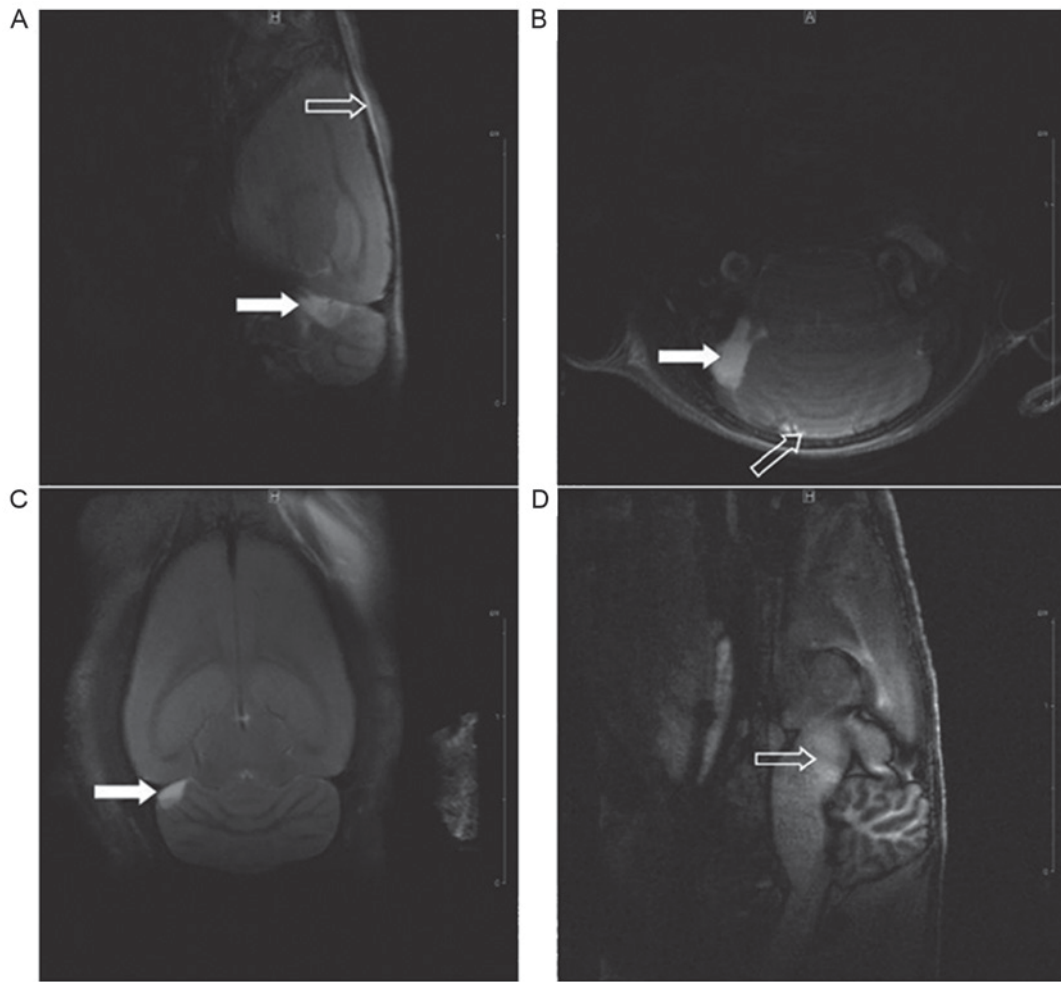


Figure 5. Magnetic resonance sequence scanning images, obtained using a Bruker Boiospec 70/30 T2 instrument, of rat heads from the experimental group at 24 h after injury. (A and B) Long T2 signal in the dorsal frontal cortex (open arrow). (A-C) The long T2 signal in the top right ventral lateral cerebellum (solid arrow) suggests laceration of brain tissue. (D) Mixed-signals exhibited at the corner of upper brain stem fibre (open arrow) are suggestive of DAI.

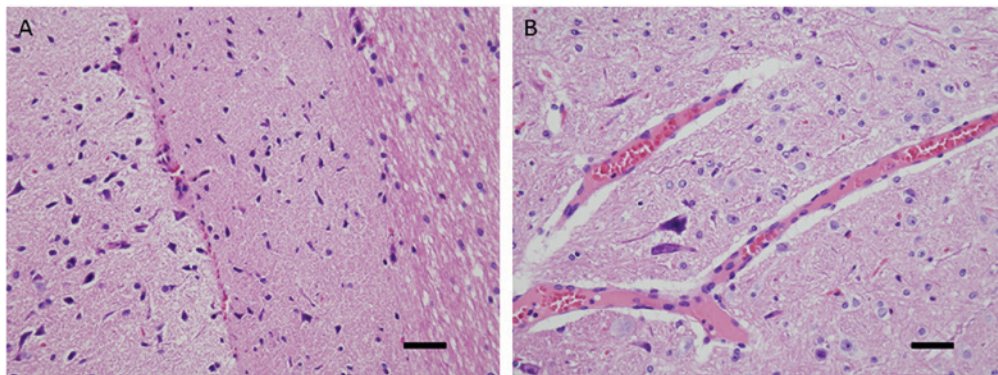


Figure 6. Brain stem tissue paraffin sections from rats were stained with hematoxylin and eosin immediately after magnetic resonance imaging at 48 h. Representative photomicrographs of the brainstem from the experimental group. (A) Triangular, hyperchromatic injured nerve cell nuclei, with a thin cell body, and (B) capillary congestion and expansion and erythrocyte sedimentation are visible. Scale bars, 100 μm .

DAI models have been obtained using tightly coupled repetitive blast-induced traumatic brain injury (11). Head swinging was used in the present study to increase the destructive effect of the shearing force and to imitate DAI in humans, with a spring to reduce excess swing amplitude in order to avoid and reduce cervical injury.

According to previous experimental results for the rat brain blast injury model (22), a detonation distance of 10 cm was set; the blast overpressure over this distance was $\sim 238.86 \pm 18.34$ kPa, which is able to cause stable bTBI in adult rats. The tension-elastic parameters of the self-made spring were measured to obtain a reference for replication of

the model. Due to the anatomical features of the brain stem, a wide radius range was expected for swinging in the sagittal plane, with an increased line speed causing an increase in the corresponding generated shear stress. Furthermore, the direction of loading (i.e., the direction of the force and the swing) was perpendicular to the longitudinal axis of the vast majority of the brain stem fibres, suggesting that the brain stem is susceptible to acceleration-deceleration movement. In addition, the brain stem and the distal brain have different compositions, resulting in large differences in their weight and density (29); thus, when the brain stem and distal brain were subjected to identical external forces, different speeds would result, thus generating shear stress. These findings indicate that shear stress was an important factor for injury in the present DAI model.

To the best of our knowledge, no recorded data concerning DAI caused by sagittal swing exists. In the present study, injury was induced through head tilt and biomechanical parameters were compared. However, Margulies *et al* (31) measured the threshold of the mechanical parameters of baboon head tilt-induced DAI as an angular velocity of 260 rad/sec and an angular acceleration of 100 krad/sec², which suggested that the lower the weight of the brain tissue, the higher the speed of the angular velocity and angular acceleration required to cause injury. In addition, Maxwell *et al* (32) measured the angular acceleration of DAI in the baboon model as 100–200 krad/sec². Furthermore, using the DAI model established through rat head tilt, with an angular velocity of 801.27 rad/sec and an angular acceleration of 204.4 krad/sec², Xiao-Sheng *et al* (21) measured the brain surface speed as 6.010±0.078 m/sec, with a turning radius of ~0.0075 m. The maximum angular velocity of the present model was 248 rad/sec, and the maximum angular acceleration was ~212 krad/sec². As the swing radius at the sagittal plane was larger than the radius of the tilt swing, and the intensity of the swing was no less than that observed in the models described above, the present established model may be considered reliable.

As no clear clinical diagnostic criteria of DAI exist at present, assessment of the injury in the present study was based on the observation of three relevant indicators of rats after injury: Clinical manifestations, MRI imaging and the pathological examination of brain tissue. Regarding the clinical manifestations, in addition to the manifestations of bTBI, such as respiratory arrest and convulsions in the limbs, there were 12 cases (75%) in the experimental group in which the duration from the beginning of anaesthesia to the recovery of the corneal reflex was >12 h, which are characteristic symptoms consistent with the clinical manifestations of DAI (30). MRI imaging results of rat brains in the experimental group indicated two major types of injury, namely cortical contusions and brain stem injury. The former may reflect the conductance of the blast shock wave through the scalp and skull to reach the brain tissue, thereby causing injury. A contrecoup injury could also be observed. In the present study, brain stem injury was the primary basis for the clinical diagnosis of DAI, which was characterized by mixed signals on the upper brain stem and clear turns in the fibres during acceleration or deceleration, which generated shearing stress and resulted in the injury and fracture of fibres. The test results obtained at different time

points revealed abnormal brain signals in the injured area at 2 h after injury; however, signal changes were most evident at 24 h after injury, and no significant changes were observed between 24 and 48 h after injury. The present results revealed that changes in the signal intensity in the injured area peaked at 24 h after the injury, with no fading, even at 48 h after the injury, which was consistent with the clinical congestion and swelling of the brain tissue affected by DAI. Brain pathology results at 48 h after injury demonstrated characteristic pathological changes of DAI. In conclusion, 14 cases (87.5%) in the experimental rat group were indicated to exhibit blast DAI, and no DAI was observed in the rats from the control group. The frequencies of categorical variables were compared using Pearson χ^2 or Fisher's exact test, when appropriate. A value of $P < 0.05$ was considered significant. The experimental design provided a stable model of rat blast DAI.

Several disturbance factors, including individual differences among animals, the blast environment and the impact of anaesthesia, existed in this model. To increase the credibility of the results, rats that were the same age, a fixed weight, and had a fixed feeding method were used. Standard atmospheric pressure and room temperature (22°C), with no noise disturbances, and a reduction of the influence of other controllable factors including, light, humidity and airflow, were set as a unified environment for the blast. Although intraperitoneal anaesthesia may affect result, the application of anaesthesia is essential to ensure the accurate exposure of the injury site to the blast at a specific distance and direction.

Some potential reasons for variability of the brain damage include i) uneven local pressure, ii) thermal damage and iii) fine fragment injury. The present model may be improved in two ways: The addition of another stable shock wave-generating source, with adjustable pressure and temperature settings, to replace the electric detonators used in this study, and the use of a special helmet to partially protect the head of the rat.

In conclusion, although previous studies of bTBI have demonstrated that DAI is a significant outcome, and various animal models have been established in accordance with the complicated mechanism of DAI, these models are not widely accepted in the field of neurology. Currently, there is no standard animal model for DAI. Although it does not represent simple DAI injury, the model developed in the present study may be useful for research regarding bTBI and DAI. Under the appropriate protection, the DAI occurrence rate remained high (87.5%) in the present model, and bTBI is likely to occur with DAI in real-life settings. In further research, remote craniocerebral and systemic exposure injuries with partial protection of the head and exposure of the trunk will be examined to compare brain electrical activity, cerebral blood flow, brain water content, intracranial pressure changes and immunohistochemical changes to further explore the specific mechanisms of brain blast injury and improve understanding of the blast characteristics of DAI. The present findings may have useful applications in clinical diagnosis and treatment, and the development of protective equipment.

Acknowledgements

The authors would like to thank Mr Shoucheng Huang (Chengdu New Innovation Sci-Tech Co., Ltd., Chengdu,

China), Professor Lu Min, Dr Li Yunming (General Hospital of People's Liberation Army Chengdu Military Region, Chengdu, China) and Dr Kang Jianyi (The Sixth Research Center of the Institute of Surgery Research, Third Military Medical University, Chongqing, China) for their excellent technical support.

Funding

The present study was supported by the Key Medical Grant of 11th five years' plan from The Chinese People's Liberation Army (grant no. 08Z011), the National Basic Research Program of China (grant no. 2011CB935800), the Public Health Training Program of the Capital (grant no. Z151100003915125) and the National Natural Science Foundation of China (grant no. 31770386).

Availability of data and materials

The datasets used and/or analyzed during the current study are available from the corresponding author on reasonable request.

Authors' contributions

JHZ performed the model preparation and was a major contributor in writing the manuscript. JWG designed and supervised the experiment. BCL performed blast waves measurement. FBG performed magnetic resonance imaging T2 sequence head scanning. XML measured the biomechanical parameters of the sagittal head swing. SJC performed pathological examinations of the brain tissue. All authors read and approved the final manuscript.

Ethics approval and consent to participate

The animal use protocol was reviewed and approved by the Institutional Animal Care and Use Committee (IACUC) of Sichuan University.

Consent for publication

Not applicable.

Competing interests

The authors declare that they have no conflict of interests.

References

- Benzinger TL, Brody D, Cardin S, Curley KC, Mintun MA, Mun SK, Wong KH and Wrathall JR: Blast-related brain injury: Imaging for clinical and research applications: Report of the 2008 st. Louis workshop. *J Neurotrauma* 26: 2127-2144, 2009.
- Zhao Y and Wang ZG: Blast-induced traumatic brain injury: A new trend of blast injury research. *Chin J Traumatol* 18: 201-203, 2015.
- Heinzelmann M, Reddy SY, French LM, Wang D, Lee H, Barr T, Baxter T, Mysliwiec V and Gill J: Military personnel with chronic symptoms following blast traumatic brain injury have differential expression of neuronal recovery and epidermal growth factor receptor genes. *Front Neurol* 5: 198, 2014.
- Valiyaveetil M, Alamneh YA, Miller SA, Hammamieh R, Arun P, Wang Y, Wei Y, Oguntayo S, Long JB and Nambiar MP: Modulation of cholinergic pathways and inflammatory mediators in blast-induced traumatic brain injury. *Chem Biol Interact* 203: 371-375, 2013.
- Courtney A and Courtney M: The complexity of biomechanics causing primary blast-induced traumatic brain injury: A review of potential mechanisms. *Front Neurol* 6: 221, 2015.
- Edwards MJ, Lustik M, Carlson T, Tabak B, Farmer D, Edwards K and Eichelberger M: Surgical interventions for pediatric blast injury: An analysis from Afghanistan and Iraq 2002 to 2010. *J Trauma Acute Care Surg* 76: 854-858, 2014.
- Chen YC, Smith DH and Meaney DF: In-vitro approaches for studying blast-induced traumatic brain injury. *J Neurotrauma* 26: 861-876, 2009.
- Wang Y, Wei Y, Oguntayo S, Wilkins W, Arun P, Valiyaveetil M, Song J, Long JB and Nambiar MP: Tightly coupled repetitive blast-induced traumatic brain injury: Development and characterization in mice. *J Neurotrauma* 28: 2171-2183, 2011.
- Svetlov SI, Prima V, Kirk DR, Gutierrez H, Curley KC, Hayes RL and Wang KK: Morphologic and biochemical characterization of brain injury in a model of controlled blast overpressure exposure. *J Trauma* 69: 795-804, 2010.
- Ling G, Bandak F, Armonda R, Grant G and Ecklund J: Explosive blast neurotrauma. *J Neurotrauma* 26: 815-825, 2009.
- Risling M, Plantman S, Angeria M, Rostami E, Bellander BM, Kirkegaard M, Arborelius U and Davidsson J: Mechanisms of blast induced brain injuries, experimental studies in rats. *Neuroimage* 54 (Suppl 1): S89-S97, 2011.
- Bell MK: Standardized model is needed to study the neurological effects of primary blast wave exposure. *Mil Med* 173: v-viii, 2008.
- Zhao Y, Zhao Y, Zhang M, Zhao J, Ma X, Huang T, Pang H, Li J and Song J: Inhibition of TLR4 signalling-induced inflammation attenuates secondary injury after diffuse axonal injury in rats. *Mediators Inflamm* 2016: 4706915, 2016.
- Gennarelli TA, Thibault LE, Tipperman R, Tomei G, Sergot R, Brown M, Maxwell WL, Graham DI, Adams JH, Irvine A, *et al*: Axonal injury in the optic nerve: A model simulating diffuse axonal injury in the brain. *J Neurosurg* 71: 244-253, 1989.
- Dixon CE, Lyeth BG, Povlishock JT, Findling RL, Hamm RJ, Marmarou A, Young HF and Hayes RL: A fluid percussion model of experimental brain injury in the rat. *J Neurosurg* 67: 110-119, 1987.
- Marmarou A, Foda MA, van den Brink W, Campbell J, Kita H and Demetriadou K: A new model of diffuse brain injury in rats. Part I: Pathophysiology and biomechanics. *J Neurosurg* 80: 291-300, 1994.
- Wang HC, Duan ZX, Wu FF, Xie L, Zhang H and Ma YB: A new rat model for diffuse axonal injury using a combination of linear acceleration and angular acceleration. *J Neurotrauma* 27: 707-719, 2010.
- Nishimoto T and Murakami S: Relation between diffuse axonal injury and internal head structures on blunt impact. *J Biomech Eng* 120: 140-147, 1998.
- Garman RH, Jenkins LW, Switzer RC III, Bauman RA, Tong LC, Swauger PV, Parks SA, Ritzel DV, Dixon CE, Clark RS, *et al*: Blast exposure in rats with body shielding is characterized primarily by diffuse axonal injury. *J Neurotrauma* 28: 947-959, 2011.
- Säljö A, Bao F, Haglid KG and Hansson HA: Blast exposure causes redistribution of phosphorylated neurofilament subunits in neurons of the adult rat brain. *J Neurotrauma* 17: 719-726, 2000.
- Xiao-Sheng H, Sheng-Yu Y, Xiang Z, Zhou F and Jian-ning Z: Diffuse axonal injury due to lateral head rotation in a rat model. *J Neurosurg* 93: 626-633, 2000.
- Cheng J, Gu J, Ma Y, Yang T, Kuang Y, Li B and Kang J: Development of a rat model for studying blast-induced traumatic brain injury. *J Neurol Sci* 294: 23-28, 2010.
- Elder GA, Gama Sosa MA, De Gasperi R, Stone JR, Dickstein DL, Haghghi F, Hof PR and Ahlers ST: Vascular and inflammatory factors in the pathophysiology of blast-induced brain injury. *Front Neurol* 6: 48, 2015.
- Huo J, Liu J, Wang J, Zhang Y, Wang C, Yang Y, Sun W and Xu S: Early hyperbaric oxygen therapy inhibits aquaporin 4 and adrenocorticotropic hormone expression in the pituitary gland of rabbits with blast-induced craniocerebral injury. *Neural Regen Res* 7: 1729-1735, 2012.
- Gennarelli TA, Thibault LE, Adams JH, Graham DI, Thompson CJ and Marcincin RP: Diffuse axonal injury and traumatic coma in the primate. *Ann Neurol* 12: 564-574, 1982.
- Meythaler JM, Peduzzi JD, Eleftheriou E and Novack TA: Current concepts: Diffuse axonal injury-associated traumatic brain injury. *Arch Phys Med Rehabil* 82: 1461-1471, 2001.

27. Hill CS, Coleman MP and Menon DK: Traumatic axonal injury: Mechanisms and translational opportunities. *Trends Neurosci* 39: 311-324, 2016.
28. Siedler DG, Chuah MI, Kirkcaldie MT, Vickers JC and King AE: Diffuse axonal injury in brain trauma: Insights from alterations in neurofilaments. *Front Cell Neurosci* 8: 429, 2014.
29. Fijalkowski RJ, Stemper BD, Pintar FA, Yoganandan N, Crowe MJ and Gennarelli TA: New rat model for diffuse brain injury using coronal plane angular acceleration. *J Neurotrauma* 24: 1387-1398, 2007.
30. Ma J, Zhang K, Wang Z and Chen G: Progress of research on diffuse axonal injury after traumatic brain injury. *Neural Plast* 2016: 9746313, 2016.
31. Margulies SS, Thibault LE and Gennarelli TA: Physical model simulations of brain injury in the primate. *J Biomech* 23: 823-836, 1990.
32. Maxwell WL, Watt C, Graham DI and Gennarelli TA: Ultrastructural evidence of axonal shearing as a result of lateral acceleration of the head in non-human primates. *Acta Neuropathol* 86: 136-144, 1993.



This work is licensed under a Creative Commons Attribution-NonCommercial-NoDerivatives 4.0 International (CC BY-NC-ND 4.0) License.